

## Surface Specularity as an Indicator of Shock-Induced Solid-Liquid Phase Transitions in Tin

G. D. Stevens <sup>1</sup>, S. S. Lutz <sup>1</sup>, B. R. Marshall <sup>1</sup>, W. D. Turley <sup>1</sup>, L. R. Veaser <sup>1, 2</sup>,  
R. S. Hixson <sup>2</sup>, B. J. Jensen <sup>2</sup>, P. A. Rigg <sup>2</sup>, M. D. Wilke <sup>2</sup>

<sup>1</sup> National Security Technologies, LLC, Special Technologies Laboratory, Santa Barbara, CA 93111

<sup>2</sup> Los Alamos National Laboratory, Los Alamos, NM 87545

**Abstract.** When highly polished metal surfaces melt upon release after shock loading, they exhibit features that suggest significant surface changes accompany the phase transition. The reflection of light from such surfaces changes from specular (pre-shock) to diffuse upon melting. Typical of this phenomenon is the loss of signal light in velocity interferometer system for any reflector (VISAR) measurements, which usually occurs at pressures high enough to melt the free surface. Unlike many other potential material phase-sensitive diagnostics (e.g., reflectometry, conductivity), that show relatively small (1%–10%) changes, the specularity of reflection provides a more sensitive and definitive (>10x) indication of the solid-liquid phase transition. Data will be presented that support the hypothesis that specularity changes indicate melt in a way that can be measured easily and unambiguously.

**Keywords:** tin, melt, phase change diagnostic, PDV, specularity

**PACS:** 62.50.+p, 47.40.Nm, 78.68.+M

## INTRODUCTION

It is apparent from studies of shocked tin that when a free surface melts upon shock release, as it does above about 22 GPa [1], the surface ceases to reflect light in the same way as when the tin release is to a solid. For example, velocity interferometer system for any reflector (VISAR) measurements fail [2, 3], and the reflectivity of the shocked sample changes greatly [4]. In this paper, we report on experiments to understand these changes. We have developed a simple, definitive melt diagnostic based on changes in optical backscattering at melt.

## EXPERIMENTS

Shock waves for this work were driven by high explosive (HE) cylinders of 12.7 mm diameter and 12–12.7 mm thickness. A 1.5–4 mm thick, 25-mm-diameter tin sample was

placed in contact with the HE. A schematic diagram of the explosive and sample is shown in the paper by Lutz [5].

When shocked using PBX-9501 explosive, a 2-mm-thick tin sample reaches a pressure of 28–30 GPa at the free surface, and it is estimated that the sample will be largely melted when the shock wave releases into air. For thicker samples, the release pressures are lower because of the Taylor wave decay of the HE shock drive, and thus we can use thicker samples to reduce the melt fraction at the surface. Using Detasheet HE, which is less energetic than PBX-9501, the shocked tin remains solid. All of the shocks have a small convex curvature at the free surface because the HE is detonated at the center. In the sample, there is a region of high strain around 6 mm from the center, which is at the diameter of the HE and outside the area of interest for most of our work.

## OPTICAL SCATTERING EXPERIMENTS

We started with a study of the characteristics of a laser beam reflected from a polished metal sample at shock breakout (SBO). We positioned an  $f/1$  Fresnel lens with the tin surface at its focal point, as shown schematically in Fig. 1. A framing camera imaged the lens (not the tin sample beyond it). Light from a laser was focused through the lens to a spot on the tin, and we looked for changes in the angular dependence of the reflected laser beam. Below melt (Fig. 2a), the reflected laser spot remained nearly unchanged for many microseconds. When the tin melted upon shock release, the reflected intensity in the central spot decreased significantly, and the Fresnel lens filled with scattered light; see Fig. 2b. We concluded that upon melt the shocked tin surface suddenly changes from specular to diffusely scattering and, as a result, the reflected light fills the Fresnel lens.

We repeated the experiment using polarized laser light and a crossed polarizer covering half of the Fresnel lens; the results indicated that the post-melt scattering effectively scrambled the polarization. We believe that this depolarization is evidence that after melt most of the reflected light scattered more than once at the surface because such depolarization occurs only for deeply-rough surfaces or volume scatterers.

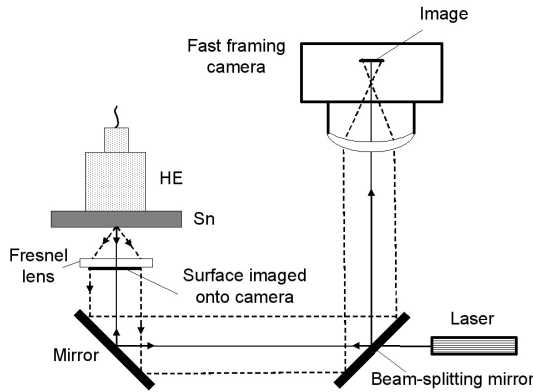


**Figure 1.** Schematic of Fresnel lens experiment. A tin sample is placed at the focal point of the lens. Light from a laser (solid line) is reflected (solid line) or scattered (dashed lines) from the tin. Mirrors relay the image of the lens out of the explosive-containment vessel to a high-speed framing camera, which images the lens at nine times bracketing SBO.

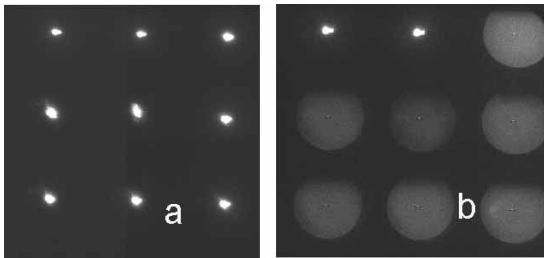


**Figure 2.** Framing camera images of the lens in Fig. 1 indicate specular reflections below melt (a) and diffuse scattering above melt (b). Frames are at 300-ns-intervals. They begin in the upper left and proceed clockwise, ending in the center. SBO is between frames 2 and 3.

## OPTICAL BACKSCATTER DIAGNOSTIC

To focus on the scattering at large angles we fabricated a diagnostic comprised of three Photon Doppler Velocimeter (PDV) [6] probes. One probe was aimed normal to the sample surface, and two were at angles of  $30^\circ$  and  $60^\circ$ . The probes were small, graded-index collimators 8 mm from the center of the surface. Laser light at 1550 nm was split with fiber-optic couplers and sent into each of the probes on single-mode optical fibers. Scattered light returning to the three probes and fibers was combined in the couplers and sent to the homodyne mixer. The three probes illuminated different, slightly-offset spots so that they would not cross-talk. The specular return beam at  $0^\circ$  was large enough in diameter to allow us to offset

that probe slightly to avoid the huge specular signal at  $0^\circ$ . The system required 200 mW of laser output power to obtain adequate return signals.

Fourier analysis of three shots produced the spectrograms shown in Fig. 3. The Fourier frequencies in the scattered spectra appear as darkened regions that denote velocity vs. time. Different probe signals have different apparent velocities that scale as the cosine of the angle from normal incidence.

The upper graph shows the results when the tin was shocked using PBX-9501 to melt on release. The three waveforms are identified, from top to bottom, as resulting from backscattering at  $0^\circ$ ,  $30^\circ$ , and  $60^\circ$ . From the velocity of the  $0^\circ$  waveform, 1990 m/s, we know that the peak sample stress at the free surface just before SBO was 29.6 GPa. The signals end when the sample begins to impact the probes at 1.5–4  $\mu$ s after SBO. The  $60^\circ$  probe is closest to the sample, and is the first to be impacted.

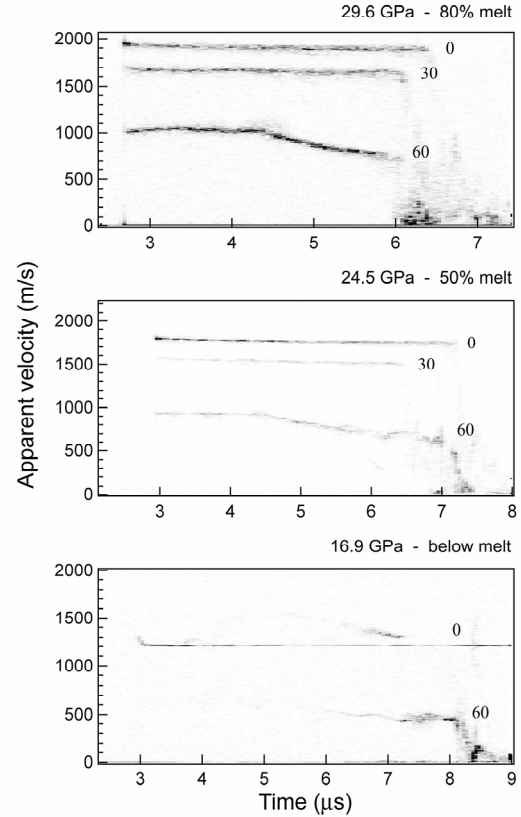


**Figure 3.** Spectrograms for shocked tin at three different melt conditions. Apparent velocity is the free surface velocity times the cosine of the angle of the probe relative to normal. Three collection angles are present for each experiment, 0°, 30°, and 60°. Shock breakouts are between 2.7 and 3.0  $\mu\text{s}$  on the graphs, and probes were impacted by the samples between 6 and 9  $\mu\text{s}$ .

To understand the melt conditions we used the one-dimensional hydrodynamic code WONDY [7] to do numerical simulations. We used a 3-phase EOS (equation of state) subroutine written by Hayes [8] and the EOS parameters [1]. To partially compensate for the two-dimensionality of our problem, we reduced the energy of the HE drive until we matched the observed free-surface velocities. These calculations predicted that for this case the tin was about 80% melted near the surface.

The center graph of Fig. 8 is for a 3-mm-thick tin sample. Here, the free surface velocity is 1.73 km/s and the shock stress is 24.5 GPa, slightly above melt threshold. The numerical simulations predict a melt fraction of about 50% near the surface. At early times, the off-normal probes returned relatively weaker signals than at higher stresses, but they are still unambiguously present.

The bottom graph is for a 2-mm-thick tin sample shocked with Detasheet to a stress somewhat below melt. The 0° signal shows a velocity drop from 1.30 to 1.21 km/s immediately after SBO, corresponding to a change in stress from 16.9 to 15.5 GPa. This change sig-

nifies that the material had significant strength, of order 0.7 GPa, and the sample remained solid. The 30° probe signal is not visible, and the 60° signal only becomes visible at about 3  $\mu$ s after SBO when it is impacted by the moving surface. We interpret these signals as evidence that the surface did not become diffusely reflecting at SBO, as occurred above melt.

Also apparent in Fig. 3 is the observation that the spread in the Doppler velocities measured by each probe is much greater above melt than below. By repeating the Fourier analysis with large time bins we can estimate the inherent frequency widths of the PDV lines and therefore also the reflecting-surface velocity spreads. Fig. 4 shows the results for several experiments between 16 and 32 GPa. The velocity spectrum for each probe was fit with a Gaussian at each point in time, and the resulting full-widths at half maximum (FWHM) are plotted versus shock stress. At 28-30 GPa, the velocities in a given PDV line have a range of about 35 m/s, nearly 2% of the free surface velocity. This is enough to destroy a VISAR signal if the VISAR fringe constant is such that there will be a few fringes for this velocity. At 16 GPa the spread is about 5 m/s, which is limited by the choice of sliding fast Fourier transform window size. Just above melt, the velocity spread increases with shock stress.

Two further observations are relevant. First, the spectrogram line widths fluctuate in time. The error bars in Fig. 4 represent the standard deviation of the fluctuations in the FWHM over the first recorded microsecond. Second, for high-pressure shots (above 26 GPa), the 30° and 60° lines have approximately the same width as the 0° lines. A possible interpretation is that the reflecting material at the free surface has about as much variation in transverse velocity as in the forward direction.

## SUMMARY

We have built a dynamic melt diagnostic based on free-surface reflectivity changes from specular to diffuse. It is relatively inexpensive and easy to field, and since it does not rely on the disappearance of reflected light, it is reasonably unambiguous and definitive. The diagnostic uses three fiber-optic probes with inexpensive lenses and a single PDV detector and recording channel to measure the surface velocities. It requires some additional testing to see how well it will function for planar shots and for unpolished samples.

It is evident that the major cause of the reflectivity changes for a free surface at melt, as seen by some workers [4], is not absorption changes in the melted material but rather large-angle scattering caused by roughening of the surface. Our measurements of the appearance of off-normal optical backscattering with increasing shock stress agree well with the measured loss of reflectivity in [4].

## ACKNOWLEDGEMENTS

We wish to thank Michael Grover for his technical assistance with explosive experiments.

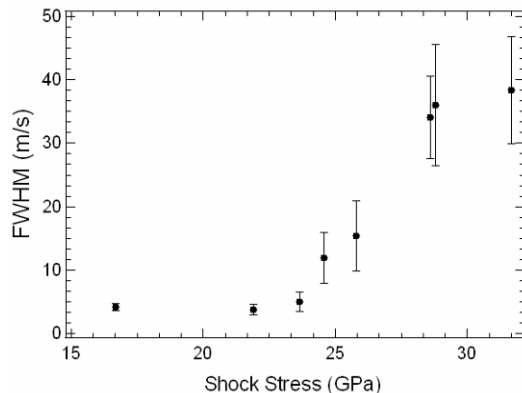


**Figure 4.** Spread in the measured surface velocities as a function of shot pressure. Velocity spreads were obtained from the widths of the Fourier transform lines in the PDV experiments. Melt threshold is about 23 GPa.

This manuscript has been authored by National Security Technologies, LLC, under Contract No. DE-AC52-06NA25946 with the U.S. Department of Energy. The United States Government retains and the publisher, by accepting the article for publication, acknowledges that the United States Government retains a non-exclusive, paid-up, irrevocable, world-wide license to publish or reproduce the published form of this manuscript, or allow others to do so, for United States Government purposes.

## REFERENCES

- 1) Mabire, C. and Hereil, P. L., "Shock induced polymorphic transition and melting of tin," Shock Compression of Condensed Matter – 1999 (Ed. by M. D. Furnish, L. C. Chhabildas, and R. S. Hixson), American Institute of Physics, p. 93-96 (2000).
- 2) Holtkamp, D. B., et al., "A survey of high explosive-induced damage and spall in selected metals using proton radiography," CP706, Shock Compression of Condensed Matter – 2003, (Ed. by M. D. Furnish, Y. M. Gupta, and J. W. Forbes), American Institute of Physics, p. 477-482 (2004).
- 3) de Resseguier, T., et al., "Experimental investigation of liquid spall in laser shock-loaded tin," J. Appl. Phys. 101, 031506 (2007).
- 4) Elias, P., Chapron, P., and Laurent, B., "Detection of melting in release for a shock-loaded tin sample using the reflectivity measurement method," Optics Comm. 66, 100 (1983).
- 5) Lutz, S. S., Turley, W. D., Rightley, P. M., and Primas, L. E., "Gated IR images of shocked surfaces," Shock Compression of Condensed Matter - 2001, (Ed. by M. D. Furnish, N. N. Thadhani, and Y. Horie), American Institute of Physics, p. 1239-1242 (2002).
- 6) Strand, O. T., et al., "Compact system for high-speed velocimetry using heterodyne techniques," Rev. Sci. Instrum. 77, 083108 (2006).
- 7) Kipp, M. E. and Lawrence, R. J., "WONDY V - A one-dimensional finite difference wave propagation code," Sandia National Laboratories Report SAND81-0930 (1982).
- 8) Hayes, D. B., "Wave propagation in a condensed medium with N transforming phases: Application to Solid-I-solid-II-liquid bismuth," J Appl. Phys. 46, p. 3438 (1975); D. B. Hayes, Private Communication (2005).

